Published in final edited form as:
Mol Microbiol. 2014 January ; 91(1): 57–65. doi:10.1111/mmi.12439.

Stable micron-scale holes are a general feature of canonical holins

Christos G. Savva[1,2,5], **Jill S. Dewey**[4,6], **Samir H. Moussa**[1,3,7], **Kam H. To**[1], **Andreas Holzenburg**[1,2,4], and **Ry Young**[3,4,*]

[1]Department of Biology, Texas A&M University, College Station, Texas 77843-3258

[2]Microscopy and Imaging Center, Texas A&M University, College Station, Texas 77843-2257

[3]Center for Phage Technology, Texas A&M University, College Station, Texas 77843-2128

[4]Department of Biochemistry and Biophysics, Texas A&M University, College Station, Texas 77843-2128

Summary

At a programmed time in phage infection cycles, canonical holins suddenly trigger to cause lethal damage to the cytoplasmic membrane, resulting in the cessation of respiration and the non-specific release of pre-folded, fully active endolysins to the periplasm. For the paradigm holin S105 of lambda, triggering is correlated with the formation of micron-scale membrane holes, visible as interruptions in the bilayer in cryo-electron microscopic images and tomographic reconstructions. Here we report that the size distribution of the holes is stable for long periods after triggering. Moreover, early triggering caused by an early lysis allele of *S105* formed approximately the same number of holes, but the lesions were significantly smaller. In contrast, early triggering prematurely induced by energy poisons resulted in many fewer visible holes, consistent with previous sizing studies. Importantly, the unrelated canonical holins P2 Y and T4 T were found to cause the formation of holes of approximately the same size and number as for lambda. In contrast, no such lesions were visible after triggering of the pinholin $S^{21}68$. These results generalize the hole formation phenomenon for canonical holins. A model is presented suggesting the unprecedentedly large size of these holes is related to the timing mechanism.

Introduction

Holins are an extremely diverse group of small phage-encoded membrane proteins that control the length of the phage infection cycle (Young, 1992, Wang *et al.*, 2000, Young, 2002). The holin proteins accumulate harmlessly in the cytoplasmic membrane throughout the morphogenesis period until suddenly forming lethal, non-specific membrane lesions or holes, in the bilayer, allowing the release of the phage endolysin to attack the cell wall. This event, called holin triggering, is allele-specific but can be prematurely induced by partial

*Corresponding author; ryland@tamu.edu, Phone:979-845-2087, Fax: 979-862-4718.
[5]current address: MRC Laboratory of Molecular Biology, Cambridge, CB2 0QH
[6]current address: Department of Biology, University of Saint Thomas, Houston, Texas 77006
[7]current address: Department of Microbiology and Immunobiology, Harvard Medical School, 4 Blackfan Circle, Boston, MA 02115

depolarization of the membrane (Doermann, 1952, Young, 1992). Holins can be further classified into two fundamentally different types: canonical holins and pinholins. Canonical holins, represented by the paradigm holin S105 of phage lambda, form holes that allow the escape of a pre-folded, fully active soluble endolysin from the cytoplasm into the periplasmic space. For S105, it was known that the holes were non-specific, in that they could serve unrelated endolysins (Wang et al., 2000), and very large, in that S105-mediated lysis was unaffected when the lambda endolysin R was fused to βgalactosidase, creating a chimera of ~0.5 MDa (Wang *et al.*, 2003). In contrast, the pinholins, as represented by the $S^{21}68$ protein of lambdoid phage 21, trigger to form heptameric channels of ~2 nm diameter (Pang *et al.*, 2009). Too small to allow protein release, these "pinholes" instead serve to depolarize the membrane. Pinholins require special endolysins designated SAR (signal anchor release) endolysins. Instead of relying on the holin for release to the periplasm, SAR endolysins are exported by the host *sec* system and are activated by the collapse of the membrane potential (Xu *et al.*, 2004, Park *et al.*, 2007).

Recently, the first direct images of the S105 lesion, visualized as interruptions in the bilayer, were obtained by cryo-electron microscopy (cryo-EM) (Dewey *et al.*, 2010). The holes were characterized in terms of their size and localization throughout the membrane, and cryo-electron tomography was used to create three-dimensional reconstructions of the S105 hole. The lesions were found to be of unprecedented and highly variable size, with an average diameter of ~340 nm ± 35 nm. At minimum, the existence of these "micron-scale" holes explains the previous findings of the non-specificity and capacity for release of R-βgalactosidase fusions.

Even more recently, studies with GFP fusions of the lambda holin S105 showed that triggering was correlated with a sudden redistribution of holin proteins, from a uniformly dispersed state to a small number of highly oligomeric aggregates, designated as rafts (White *et al.*, 2011). A model has been proposed in which the S105 rafts cause local depolarization of the membrane, leading then to reorganization of the rafts into holes. Thus the allele-specific variation in lysis timing stems from allelic differences in the time at which raft formation is nucleated; i.e., each *S105* allele would trigger at a critical concentration of holin within the two-dimensional context of the membrane.

Holin genes have been annotated in many phage genomes, more often than not by criteria no more robust than being small and having at least one trans-membrane domain (TMD) (Young, 1992, Wang et al., 2000, Young, 2002). Three topological classes have been described (Fig. 1). Class I holins, including the prototype lambda S105, have three TMDs, and an N-out, C-in topology. Class II holins have two TMDs, and an N-in, C-in topology. Class III holins have one TMD, and an N-in, C-out topology. Besides S105, only a few holins have been validated experimentally, including P2 Y of class I (Ziermann *et al.*, 1994, To *et al.*, 2013), the class II pinholin $S^{21}68$ (Pang et al., 2009), and the class III holin T of phage T4 (Ramanculov & Young, 2001a, Ramanculov & Young, 2001b).Of these, both P2 Y (To et al., 2013) and T4 T (Wang et al., 2003) have been shown to release the endolysin-βgalactosidase fusions after triggering in vivo.

The diversity in holin primary structure, membrane topology and hole permissivity makes it important to determine whether the micron-scale lesions observed with S105 are a common feature of holins, or unique to the lambda protein. Moreover, nothing is known about the stability or kinetics of the formation of the micron-scale holes lesions. Here we report cryo-electron microscopic studies to address this question and also to assess the dynamics, stability and correlation of hole size with triggering time. The results are discussed in terms of a model for the relationship of hole size to the temporal regulation of lysis.

Results

The lambda holin forms micron-scale holes in the context of an induced prophage

The cryo-EM experiments described earlier were done with an *E. coli* strain transformed with two separate plasmids: pS105$R_{am}Rz_{am}Rz1_{am}$, which encodes a functional holin but null endolysin and spanin proteins, and pQ, which provides the lambda Q late gene activator under inducible control (Dewey et al., 2010). A limitation of those experiments was that the lysis genes were not expressed in the context of the complete phage gene expression program. Given the unexpected and unprecedented size of the lesions formed, we wanted to be sure that the absence of the other lambda genes outside the lysis cassette was not a factor. To address this issue, we used a different strain background containing a thermo-inducible lambda prophage, λCamΔ*SR*, which, when induced provides not only the late gene activator Q but also the complete context of the lambda infection cycle. This complementation system has been extensively validated in terms of faithful representation of lysis phenotypes (Grundling *et al.*, 2000a, Grundling *et al.*, 2000b, Grundling *et al.*, 2000c, Ramanculov & Young, 2001a, Wang et al., 2003, Park *et al.*, 2006, Park et al., 2007, Pang *et al.*, 2010a, White *et al.*, 2010, White et al., 2011, To et al., 2013). *E. coli* MC4100 Δ*tonA* λCamΔ*SR* pS105$R_{am}Rz_{am}Rz1_{am}$were induced and grown up to the time of holin triggering. Cells were immediately plunge frozen in liquid ethane and imaged for the presence of membrane lesions. Cryo-EM micrographs were obtained for 52 cells (Fig 2A), in which 31, or ~60%, had visible lesions (Fig. 2B). The holes ranged in size from 86 – 989 nm, with the major size class being 200–400 nm (Fig. 2C). As before, there was no preferential location for the holes nor any correlation between hole size and hole localization (Fig. 2D). The majority of cells with holes had single visible lesions, but there were instances of multiple visible holes per cell (Fig. 2B). Due to the fact that the micrographs represent two-dimensional projections, only a small part of the cell membrane is visible in a single image. However given the geometry of the cell and the average hole size an estimate can be calculated as to the actual number of holes per cell. Consistent with previous results these cells are estimated to have an average of ~2.5 holes.

Stability and kinetics of the holes

The results obtained so far raise the question of whether the size of the S105 holes represents the actual lesion size at time of triggering, or if on average, they expanded or contracted with time. To address this question, *E. coli* MG1655 Δ*tonA* $lacI^q$ Δ*lacY* pQ pS105$R_{am}Rz_{am}Rz1_{am}$ were induced and samples were taken at various times after the time of triggering. The results clearly show that the major size class of holes was the same. In an average of ~20 cells imaged for every time point, the major hole size class was 200 – 400

nm (Fig. 3). Thus, the large holes produced by S105 triggering do not change, at least in terms of average size, after triggering. It is important to note that a proportion of the cells in the 30 min and particularly the 60 min time points was found to be undergoing lysis as evident by spillage of ribosomes. These cells were not used for the statistics, as in some cases the entire inner membrane was not visible.

We next addressed how early triggering, either prematurely induced with an energy poison, or spontaneously occurring in an early lysis mutant, affects hole formation. To this end, cells (*E. coli* MC4100 Δ*tonA* λCamΔ*SR)* expressing the missense mutants $S105_{A52I}$ and $S105_{A52F}$ (derivatives of $pS105R_{am}Rz_{am}Rz1_{am}$) were imaged. $S105_{A52I}$ and $S105_{A52F}$ are non-lytic and early lysis alleles, respectively (K. To, R. White, C. Dankenbring, J. Dewey and R. Young, unpublished). In ~50 cells expressing $S105_{A52I}$ and imaged with cryo-EM, no lesions were detected. By contrast, in cells expressing $S105_{A52F}$, which triggers at ~11 min after induction, more than 30 min earlier than the wt, approximately the same number of lesions were observed as in the wt condition (Fig. 4A). However, the sizes of the holes in cells expressing the early-lysing mutant were smaller than in cells expressing the parental *S105*, with the major size class being only 100 – 200 nm (Fig. 4B).

The pattern was strikingly different when triggering was induced prematurely by the addition of an energy poison. When cells induced for wt *S105* were prematurely triggered at 15 minutes post induction by cyanide addition, only 21 % had inner membrane lesions detectable in the cryo-EM images (Fig. 4C). Moreover, the holes that were visible were variable in size (Fig. 4D). As a control, cells expressing *Sam7* were prematurely triggered with 10 mM KCN at 30 minutes post induction, and 98% of the cells, or 49 out of 50, did not have visible lesions (data not shown). Thus early lysis resulting from the spontaneous triggering of an early lysis allele results in a qualitatively different pattern of hole formation than for either spontaneous triggering at the wt *S105* time or artificially induced, premature triggering at the same early lysis time. These results have implications for modeling the hole-formation pathway (see Discussion.)

Unrelated canonical holins also form micron-scale holes

We next wanted to know if the micron-scale holes exhibited by S105 were also formed by other canonical holins unrelated to lambda S105. For comparison, we chose P2 Y, which shares class I topology but no sequence similarity with lambda S105 (To et al., 2013), and the holin of phage T4, T, which as the founding member of the class III holin family, has completely different membrane topology, with extensive N and C-terminal domains and only a single TMD (Ramanculov & Young, 2001a, Ramanculov & Young, 2001b). Both have been genetically, physiologically and biochemically characterized and both have the signature features of holins, in terms of inducible lethality and sensitivity to premature triggering by energy poisons. Importantly, like λ S105, they have both been shown to support lysis with the R-βgalactosidase chimera. To address whether or not the permissivity of the Y and T holins, of class I and class III, respectively, was due to lesions similarly scaled to those formed by S105, isogenic plasmids in which gene *t* or gene *Y* replaced *S105* were constructed. Cells carrying these constructs (MC4100 Δ*tonA* λCamΔ*SR* with either $pYR_{am}Rz_{am}Rz1_{am}$ or $pTR_{am}Rz_{am}Rz1_{am}$) were induced, allowed to trigger, and examined

with the same cryo-EM strategy as above. Of the 62 cells induced for Y, 29, or 46%, had visible inner membrane lesions. Hole size ranged from ~114 nm to ~1.3 μm, and the major size class was 200 – 400 nm (Fig. 5A, C, D). As in the case of λ S105, Y holes were not localized to a specific region of the membrane (Fig. 5E). Similar results were obtained for T, where out of 56 cells, 19, or 34%, had inner membrane lesions. Hole size ranged from 99 nm to 704 nm, with the majority of lesions in either the <200 nm class or the 200 – 400 nm class (Fig. 5B, C, D). As mentioned above holes smaller than ~80 nm are not clearly resolved. Thus the smallest size class was actually 80 – 200 nm. In both cases, the majority of cells with holes had a single visible hole, but there were instances where cells had multiple visible holes (Fig. 5C). The actual number of holes per cell was estimated at 2 per cell for both Y and T.

These results strongly indicate that canonical holins in general form micron-scale holes when they trigger, irrespective of topological class. Moreover, it appears that the R-βgalactosidase lysis assay, which can be done in bulk culture, can be used as a simple substitute for cryo-EM studies. Also, whether or not they are encoded by temperate or virulent phages is apparently irrelevant to this molecular strategy; i.e., once a temperate phage has committed to a vegetative cycle, the holin pathway leads to the same kind of massive disruption of the cytoplasmic membrane.

The pinholin does not form micron-scale lesions

Initially, the $S^{21}68$ pinholin, known to form heptameric pinholes (Pang et al., 2009), would seem to be an unlikely candidate for the formation of micron-scale membrane lesions of the size observed for the canonical holins. However, the cryo-EM images reveal the holes as interruptions in the cytoplasmic membrane bilayer; proteinaceous structures within these interruptions would not be detectable. Recently, GFP-fusion studies have revealed that, despite the final lesion being heptameric, the triggering of $S^{21}68$ was correlated with raft formation. This raised the possibility that the micron-scale lesions might still be formed; instead of a single large hole, the lesions might be packed with the heptameric pinholes. To address this possibility, *E. coli* MC4100 Δ*tonA* λCamΔ*SR* carrying $S^{21}68$ cloned into an isogenic construct ($pS^{21}R_{am}Rz_{am}Rz1_{am}$) were induced and examined using the same methods. In 76 cells examined, there were no visible holes in the inner membranes of these cells. Presumably this is because the pinholes, which as heptameric assemblies of the 7.5 kDa $S^{21}68$ pinholin, would only be ~4 nm in total diameter (Pang et al., 2009) would be too small to be seen with our current imaging conditions unless they were aggregated to a high degree.

Discussion

The central mystery of holin function is the triggering event. Suddenly, long after the induction of holin gene expression, the cells in a synchronously induced culture stop growing, cease respiration, release cytoplasmic ions, and lose viability. This behavior is universal for all holins tested to date, irrespective of structure or membrane topology (Ramanculov & Young, 2001a, Ramanculov & Young, 2001b, To et al., 2013, Adhya *et al.*, 1971, Reader & Siminovitch, 1971, Garrett *et al.*, 1981, Bonovich & Young, 1991, Garrett

& Young, 1982). Moreover, triggering occurs at an allele-specific time, with large differences between alleles with conservative substitutions, both advancing or retarding the triggering time (Grundling et al., 2000a, Ramanculov & Young, 2001a, To et al., 2013, Zheng *et al.*, 2008, Pang et al., 2010a). In addition, triggering can be prematurely and instantly imposed by anything that causes substantial depolarization of the membrane. Finally, and most critically for the phage infection cycle, triggering allows the release of fully folded, enzymatically active endolysin across the cytoplasmic membrane. Two key experimental approaches had provided a framework for understanding these phenomena. First, triggering of the lambda holin S105 was shown to be linked to the formation of micron-scale interruptions, or holes, in the cytoplasmic membrane (Dewey et al., 2010), thus accounting for the lethal membrane effects and the ability of folded endolysin to escape the cytoplasm and attack the cell wall. In parallel, studies with S105-GFP fusions showed that spontaneous, lethal triggering of the holin was correlated with the transition of the holin from a mobile state uniformly distributed in the membrane to a state dominated by large aggregates, or rafts (White et al., 2011). Combined with other studies, these findings have led to a model for the strict timing of holin function and lethality. In this view, the S105 holins accumulate in the membrane as harmless, mobile, dimeric species until reaching an allele-specific critical (two-dimensional) concentration. At this point, nucleation of raft formation occurs, followed by aggregation of the bulk of the holin molecules into a few large rafts. It is proposed that the rafts are permeable to proton or ion flow across the bilayer, leading to local depolarization of the membrane, which in turn causes conformational changes that allow the packed holins to reorganize into the final holes, presumably lined by the most hydrophilic face of at least one of the three TMDs of S105. As envisioned, the process is inherently saltatory, in that the conversion of any one raft into a hole leads to total depolarization of the membrane and the conversion of other rafts into holes. This aspect of the model explains the universal characteristic exhibited by all holins: that they can be prematurely triggered by any event that reduces the membrane potential.

Here we further addressed aspects of these holes, in an effort to link hole formation and stability to the current model and to generalize hole-formation for other unrelated holins. The most important findings are considered in terms of their implications for the hole-formation pathway:

1. *S105 holes are stable*: The S105 holes were found to be stable in terms of average size and distribution, irrespective of time after triggering. This is consistent with the notion that hole formation is a one-time, all-or-nothing event, rather than a process of acute, localized damaged followed by spreading membrane disruption. The simplest conclusion is that after complete membrane depolarization, there is no free energy left to drive further reorganization of the hole-forming protomers.
2. *Hole size depends on holin accumulation and allele-specific triggering time.* The distribution of hole sizes showed a significant shift towards smaller diameters for an early lysis allele of *S105*. In addition, despite the fact that premature triggering, with an energy poison causes nearly instant lysis, many cells examined under these conditions did not appear to have detectable holes at all. The simplest interpretation of these data, from the perspective of the model we have proposed, is that the large

holes of >100 nm diameter are generated by mature rafts that have depolarized the membrane and undergone reorganization into holes. In this perspective, the difference between the wt S105 and the $S105_{A52F}$ mutant is that the latter nucleates raft formation at a lower (two-dimensional) critical concentration of the holin protein. The reduced size of the holes is consistent with the notion that most or all of the holin is involved in lining the lumenal walls of the lesions, so that the alleles that trigger when S105 has accumulated to a lower level must form smaller holes (see below).

In contrast, when depolarization is imposed artificially before the critical concentration is reached, holes would likely form from local micro-heterogeneities in the holin distribution throughout the membrane. Thus although the product holes will still be lethal i.e. allow release of endolysin, the average size would be expected to be much smaller. The imaging conditions used (low magnification and high defocus) as well as the thickness of the specimen itself (~1000 nm) restrict the unambiguous identification of a hole to any gap larger than ~80 nm. It should be noted that prematurely triggered *S* inductions are not permissive for lysis with the large R-βgalactosidase hybrid endolysin (Wang et al., 2003), which constitutes *in vivo* evidence that the prematurely triggered holes are on average much smaller than the mature holes, even for early lysis alleles.

3. *Micron-scale holes are a general feature of canonical holins but not pinholins.* The extreme diversity of holins extends not only to primary structure, where more than 50 different families have been identified, but also to membrane topology (Wang et al., 2000). Three other unrelated holins have been subjected to detailed physiological and molecular characterization: Y, the class I holin of phage P2; $S^{21}68$, the class II holin of lambdoid phage 21, and T, the class III holin of phage T4 (To et al., 2013, Pang et al., 2010b, Ramanculov & Young, 2001b). Two of these holins, Y and T, are canonical holins, and here we have shown that both form the micron-scale lesions comparable in size, number and distribution to those formed by S105 (Fig.5). In contrast, no lesions were observed in the membranes in which the pinholin $S^{21}68$ had triggered. Thus canonical holins and pinholins share all the features of the triggering phenomenom except the ability to release soluble endolysins from the cytoplasm and the formation of the micron-scale lesions. The simplest interpretation is thus that the huge lesions are the means by which the endolysins escape. This interpretation is supported by the fact that canonical holins are non-specific in terms of endolysin release and are capable of releasing large ~0.5 MDa β-galactosidase chimeras. In addition, recent videomicroscopy studies have shown that S105-mediated lysis occurs by a “local blow-out” at a point in the cell envelope; it is likely that the localized disruption corresponds to the region opposite the S105 hole, where the released cytoplasmic endolysin would first encounter its murein substrate. The absence of visible lesions for the pinholin $S^{21}68$ is consistent with the size of the pinholes, which are heptamers with a single TMD of each protomer lining the pinhole. A pinhole has an estimated external diameter of ~4 nm; the absence of lesions greater than 50 nm in the cryo-EM images suggests that the pinholes do not cluster to a high degree, even though $\sim 10^3$

are formed at triggering time. Moreover, these results support the notion that the requirement of pinholins for SAR endolysins to effect lysis is due to the persistence of the cytoplasmic membrane as a barrier for pre-folded proteins even after lethal action of the pinholins.

Finally, the fact that the physiological characteristics at the cellular and culture level are the same for holins and pinholins, - i.e., spontaneous allele-specific triggering at a precisely programmed time, the sensitivity to energy poisons for premature triggering, and the extreme triggering time fluctuations resulting from conservative missense changes in the TMDs - indicates that none of these phenomena are directly caused by the formation of the macroscopic holes. In fact, recent evidence indicates that the pinholin $S^{21}68$ also goes through a drastic change in subcellular distribution at the time of triggering, transitioning from a uniformly dispersed state to a more punctate, “raft” disposition; however, the rafts formed are much smaller than for S105 and presumably consist of clusters of the heptameric pinholes (Pang *et al.*, 2013).

4. *Hole structure is consistent with a holin-lined lumen.* These findings strongly indicate that the macroscopic holes are a universal feature of canonical holins. The simplest model is that in each case, the holins line the walls of the macroscopic holes. In the original case with S105, quantification of the amount of holin present at the time of triggering was shown to be consistent with this notion (Dewey et al., 2010). At an average hole diameter of ~340 nm, ~ 1 μm of total hole perimeter is present per hole, and approximately two holes are present per cell. It is estimated that S105 triggers at ~1000 molecules per cell, which, if all the holin molecules were involved, could line 1 – 3 μm of total hole perimeter. This suggests that at least two TMDs of S105 are facing the lumen of the hole. The average hole size was somewhat smaller for T, at ~270 nm. Since T has only a single TMD, an average of two holes per cell would require ~1.6 μm of perimeter-lining protein, easily within the potential of the ~4000 molecules estimated to be present at the time of triggering(Moussa *et al.*, 2012). Recently, it was shown by quantitative Western blotting that P2 Y is present at ~1300 molecules at the time of lethal triggering, also consistent with Y molecules lining the Y holes (To et al., 2013). With the imprecision of quantitative Western blotting in mind, these calculations cannot be used to rule out the possibility of moderate “honey-combing” of the macroscopic holes; i.e., that the interruptions visualized by cryo-EM consist of a cluster of holes, rather than one large one. Nevertheless, it seems clear that a substantial fraction of the holins must participate in hole formation for each of these diverse canonical holins. This opens up the possibility of using chemical approaches to map out the surfaces of the holin molecules exposed in the macroscopic holes, as was done for the $S^{21}68$ pinhole. Alternatively, the use of fusions to electron-dense protein markers (Wang *et al.*, 2011, Bouchet-Marquis *et al.*, 2012) in combination with cryo-EM could reveal the details of the distribution of the holin in these lesions.

Experimental procedures

Plasmids and strains

The plasmids used in this work were pY$R_{am}Rz_{am}Rz1_{am}$, pS105$R_{am}Rz_{am}Rz1_{am}$ (and missense mutants), p$S^{21}R_{am}Rz_{am}Rz1_{am}$, and pT$R_{am}Rz_{am}Rz1_{am}$. All of these plasmids are derivatives of pS105 (Smith *et al.*, 1998), and have ampicillin resistance, with the sequences for holins *Y*, S^{21}, and *T* in place of *S105*, and amber mutations in *R*, *Rz*, and *Rz1*. The strains used for expression were MC4100 Δ*tonA* (λCamΔ*SR*) (Smith et al., 1998) which was used for all experiments except for the S105 time-course in which case the strain MG1655 Δ*tonA* $lacI_q$ Δ*lacY* pQ (Dewey et al., 2010) was used.

Growth conditions and monitoring

Growth conditions and inductions have been described previously (Dewey et al., 2010) except when using MC4100 Δ*tonA* (λCamΔ*SR*) where holin genes were thermally induced at 42 °C for 15 min, then grown at 37 °C until samples were taken for cryo-EM. For prematurely triggered holins, KCN was added to final concentration of 10 mM and left for an additional 5 min shaking at 37 °C.

Electron microscopy

Cryo-EM was carried out as previously described (Dewey et al., 2010) . Briefly, cultures were concentrated gently by vacuum filtration with a 0.45 mm filter, and the cells were resuspended in fresh LB. Three to five microliters of this sample was applied to C-flat (CF-4/2-2C) grids that had been freshly glow-discharged and plunge frozen using an FEI Vitrobot. Grids were transferred to a Gatan 626 cryo-specimen holder and imaged on an FEI Tecnai G^2 F20 transmission electron microscope operating at an acceleration voltage of 200 kV. Images were recorded in low dose (<10 e-/$Å^2$) and zero energy loss conditions (20 eV slit) on a Gatan Ultrascan 1000 CCD camera attached to the end of a Gatan Tridiem energy filter. Interruptions of the cytoplasmic membrane along the lateral axis of the cell were calculated by measuring the line distance between the 2 points of the inner membrane at which membrane density could no longer be discerned and were found, as previously reported (Dewey et al., 2010), only in cells in which functional holin was expressed. The poles of the cells were not included in the any of the lesion measurements because the continuous cytoplasmic membrane could not be routinely followed there even in cells not exposed to holin function.

Acknowledgments

We would like to thanks Rebecca White and Ting Pang for constructing and providing some of the strains used in this study. This work was supported by PHS grant GM27099 (to RY) and by the Center for Phage Technology, an Initial University Multidisciplinary Research Initiative of Texas A&M University and Texas AgriLife.

References

Adhya, S.; Sen, A.; Mitra, S.; Hershey, AD. The Bacteriophage Lambda. Cold Spring Harbor, NY: Cold Spring Harbor Laboratory; 1971. The role of gene S; p. 743-746.

Bonovich MT, Young R. Dual start motif in two lambdoid S genes unrelated to lambda S. J Bacteriol. 1991; 173:2897–2905. [PubMed: 2019562]

Bouchet-Marquis C, Pagratis M, Kirmse R, Hoenger A. Metallothionein as a clonable high-density marker for cryo-electron microscopy. J Struct Biol. 2012; 177:119–127. [PubMed: 22068155]

Dewey JS, Savva CG, White RL, Vitha S, Holzenburg A, Young R. Micron-scale holes terminate the phage infection cycle. Proc Natl Acad Sci U S A. 2010; 107:2219–2223. [PubMed: 20080651]

Doermann AH. The intracellular growth of bacteriophages. I. Liberation of intracellular bacteriophage T4 by premature lysis with another phage or with cyanide. Journal of General Physiology. 1952; 35:645–656. [PubMed: 14898042]

Garrett J, Fusselman R, Hise J, Chiou L, Smith-Grillo D, Schulz R, Young R. Cell lysis by induction of cloned lambda lysis genes. Molecular and General Genetics. 1981; 182:326–331. [PubMed: 6457237]

Garrett JM, Young R. Lethal action of bacteriophage lambda S gene. J Virol. 1982; 44:886–892. [PubMed: 6217351]

Grundling A, Blasi U, Young R. Biochemical and genetic evidence for three transmembrane domains in the class I holin, lambda S. J Biol Chem. 2000a; 275:769–776. [PubMed: 10625606]

Grundling A, Blasi U, Young R. Genetic and biochemical analysis of dimer and oligomer interactions of the lambda S holin. J Bacteriol. 2000b; 182:6082–6090. [PubMed: 11029428]

Grundling A, Smith DL, Blasi U, Young R. Dimerization between the holin and holin inhibitor of phage lambda. J Bacteriol. 2000c; 182:6075–6081. [PubMed: 11029427]

Moussa SH, Kuznetsov V, Tran TA, Sacchettini JC, Young R. Protein determinants of phage T4 lysis inhibition. Protein Sci. 2012; 21:571–582. [PubMed: 22389108]

Pang T, Fleming TC, Pogliano K, Young R. Visualization of pinholin lesions in vivo. Proc Natl Acad Sci U S A. 2013; 110:E2054–E2063. [PubMed: 23671069]

Pang T, Park T, Young R. Mapping the pinhole formation pathway of S21. Mol Microbiol. 2010a; 78:710–719. [PubMed: 20815821]

Pang T, Park T, Young R. Mutational analysis of the S21 pinholin. Mol Microbiol. 2010b; 76:68–77. [PubMed: 20132441]

Pang T, Savva CG, Fleming KG, Struck DK, Young R. Structure of the lethal phage pinhole. Proc Natl Acad Sci U S A. 2009; 106:18966–18971. [PubMed: 19861547]

Park T, Struck DK, Dankenbring CA, Young R. The pinholin of lambdoid phage 21: control of lysis by membrane depolarization. J Bacteriol. 2007; 189:9135–9139. [PubMed: 17827300]

Park T, Struck DK, Deaton JF, Young R. Topological dynamics of holins in programmed bacterial lysis. Proc Natl Acad Sci U S A. 2006; 103:19713–19718. [PubMed: 17172454]

Ramanculov E, Young R. Functional analysis of the phage T4 holin in a lambda context. Mol Genet Genomics. 2001a; 265:345–353. [PubMed: 11361346]

Ramanculov E, Young R. Genetic analysis of the T4 holin: timing and topology. Gene. 2001b; 265:25–36. [PubMed: 11255004]

Reader RW, Siminovitch L. Lysis defective mutants of bacteriophage lambda: Genetics and physiology of S cistron mutants. Virology. 1971; 43:607–622. [PubMed: 4940968]

Smith DL, Struck DK, Scholtz JM, Young R. Purification and biochemical characterization of the lambda holin. J.Bacteriology. 1998; 180:2531–2540.

To KH, Dewey J, Weaver J, Park T, Young R. Functional analysis of a class I holin, p2 y. J.Bacteriology. 2013; 195:1346–1355.

Wang IN, Deaton JF, Young R. Sizing the holin lesion with an endolysin-βgalactosidase fusion. J.Bacteriology. 2003; 185:779–787.

Wang IN, Smith DL, Young R. Holins: the protein clocks of bacteriophage infections. Annu. Rev. Microbiol. 2000; 54:799–825. [PubMed: 11018145]

Wang Q, Mercogliano CP, Lowe J. A ferritin-based label for cellular electron cryotomography. Structure. 2011; 19:147–154. [PubMed: 21300284]

White R, Chiba S, Pang T, Dewey JS, Savva CG, Holzenburg A, Pogliano K, Young R. Holin triggering in real time. Proc Natl Acad Sci U S A. 2011; 108:798–803. [PubMed: 21187415]

White R, Tran TA, Dankenbring CA, Deaton J, Young R. The N-terminal transmembrane domain of lambda S is required for holin but not antiholin function. J Bacteriol. 2010; 192:725–733. [PubMed: 19897658]

Xu M, Struck DK, Deaton J, Wang IN, Young R. The signal arrest-release (SAR) sequence mediates export and control of the phage P1 endolysin. Proc. Natl. Acad. Sci. U.S.A. 2004; 101:6415–6420. [PubMed: 15090650]

Young R. Bacteriophage lysis: mechanism and regulation. Microbiol. Rev. 1992; 56:430–481. [PubMed: 1406491]

Young R. Bacteriophage holins: deadly diversity. J.Mol.Microbiol.Biotechnol. 2002; 4:21–36. [PubMed: 11763969]

Zheng Y, Struck DK, Dankenbring CA, Young R. Evolutionary dominance of holin lysis systems derives from superior genetic malleability. Microbiology. 2008; 154:1710–1718. [PubMed: 18524925]

Ziermann R, Bartlett B, Calendar R, Christie GE. Functions involved in bacteriophage P2-induced host cell lysis and identification of a new tail gene. J.Bacteriology. 1994; 176:4974–4984.

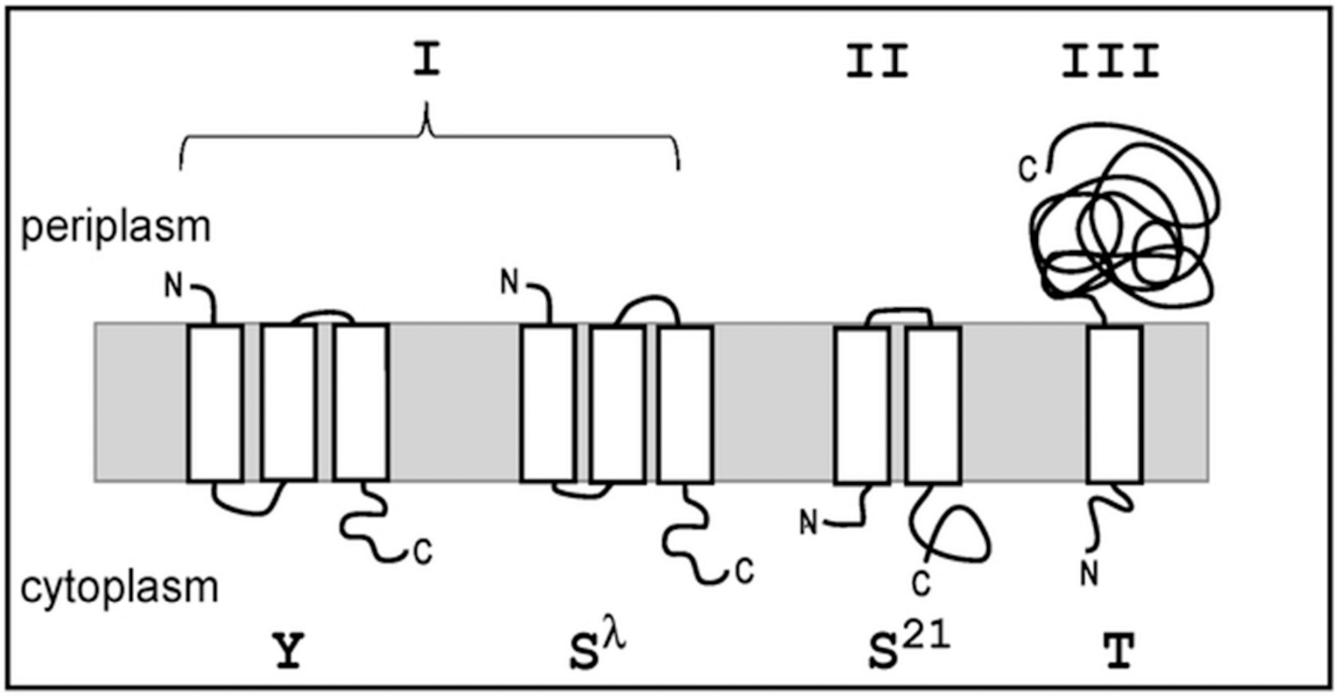

Figure 1.

Topology diagram of holin classes. Examples of each holin class are represented by the holins used in this study. Class I (P2Y and S105), class II (S^{21}68), class III (T4T).

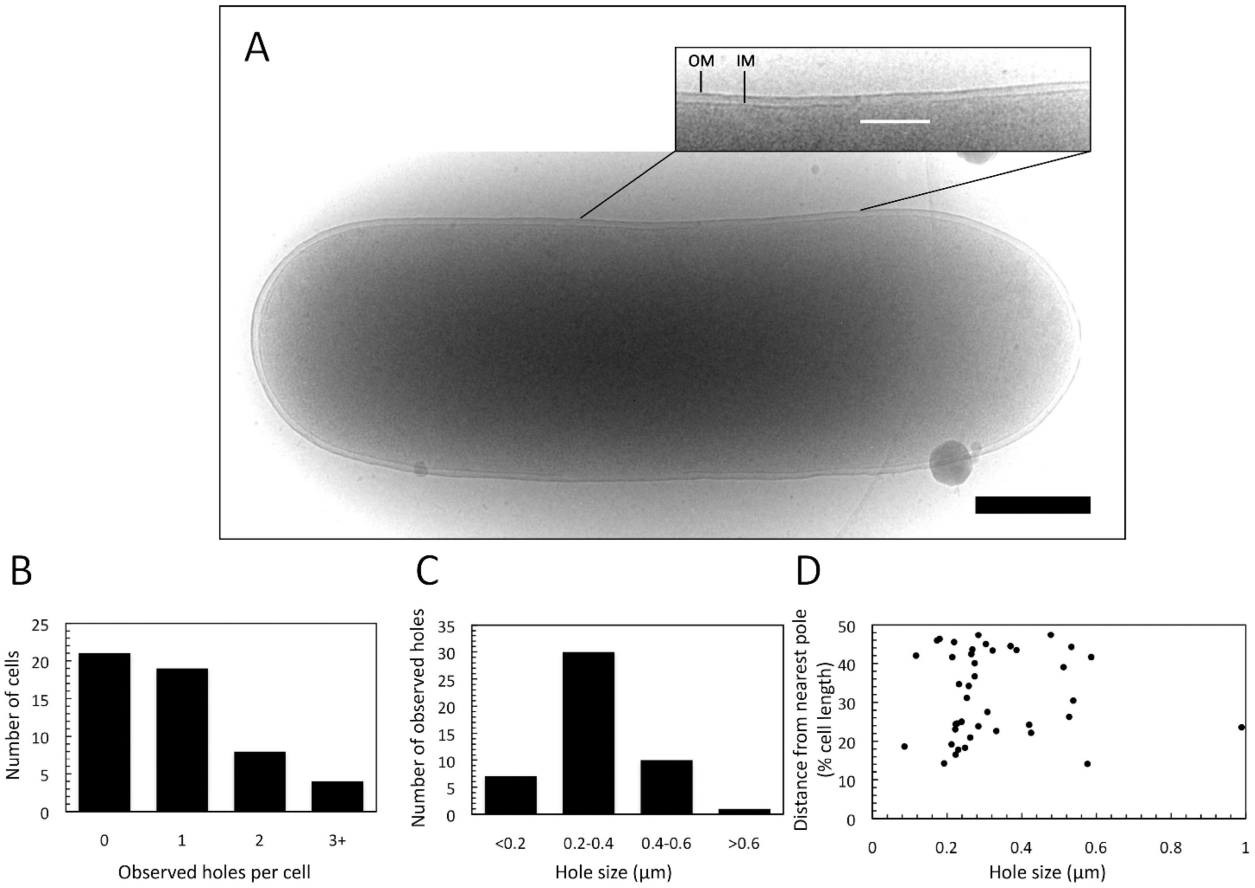

Figure 2.

Hole formation by S105 in the context of an induced prophage. A culture of *E. coli* MC4100 Δ*tonA* λCamΔ*SR* pS105$R_{am}$$Rz_{am}$$Rz1_{am}$ was thermally induced and grown until holin triggering, as monitored by the optical density of the culture. Cells were immediately plunge435 frozen in ethane and observed by cryo-TEM as described in Materials and Methods. (A) Cryo-micrograph of an *E. coli* cell bearing an S105 lesion. Inset: close-up view of the area in which a lesion is observed in the inner membrane. OM: Outer membrane. IM: Inner membrane. The white line indicates the location and extent of the lesion. Scale bar corresponds to 500 nm. (B) Number of holes/cell observed. (C) Hole size distribution. (D) Hole distance from nearest pole vs. hole size.

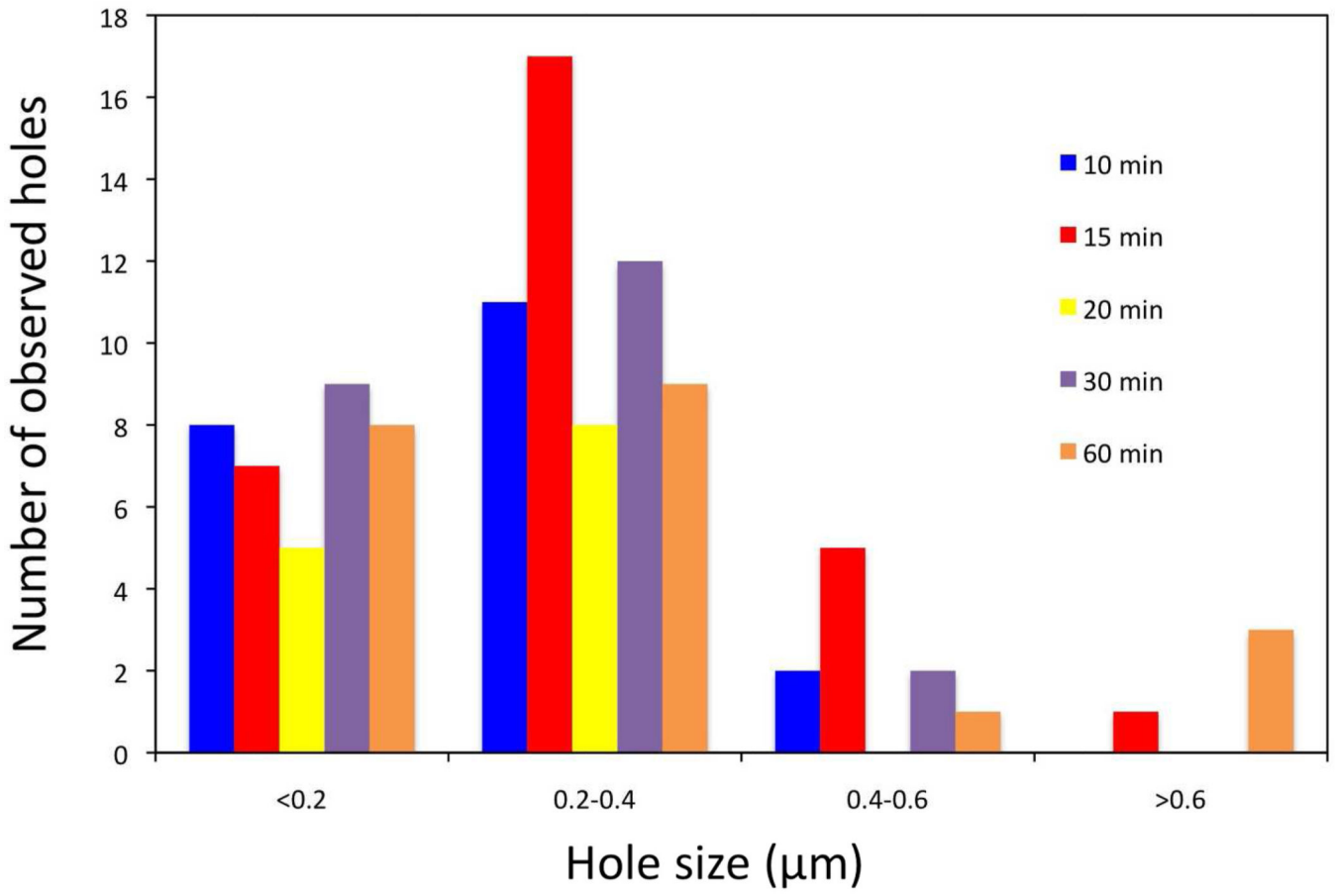

Figure 3.

Stability of the S105-derived lesions. A culture of *E. coli* MG1655 Δ*tonA lacI*^{q} Δ*lacY* pQ pS105R$_{am}$Rz$_{am}$Rz1$_{am}$ was induced with IPTG. Samples were removed for plunge freezing at the indicated times after holin triggering and analyzed as described for Fig. 2.

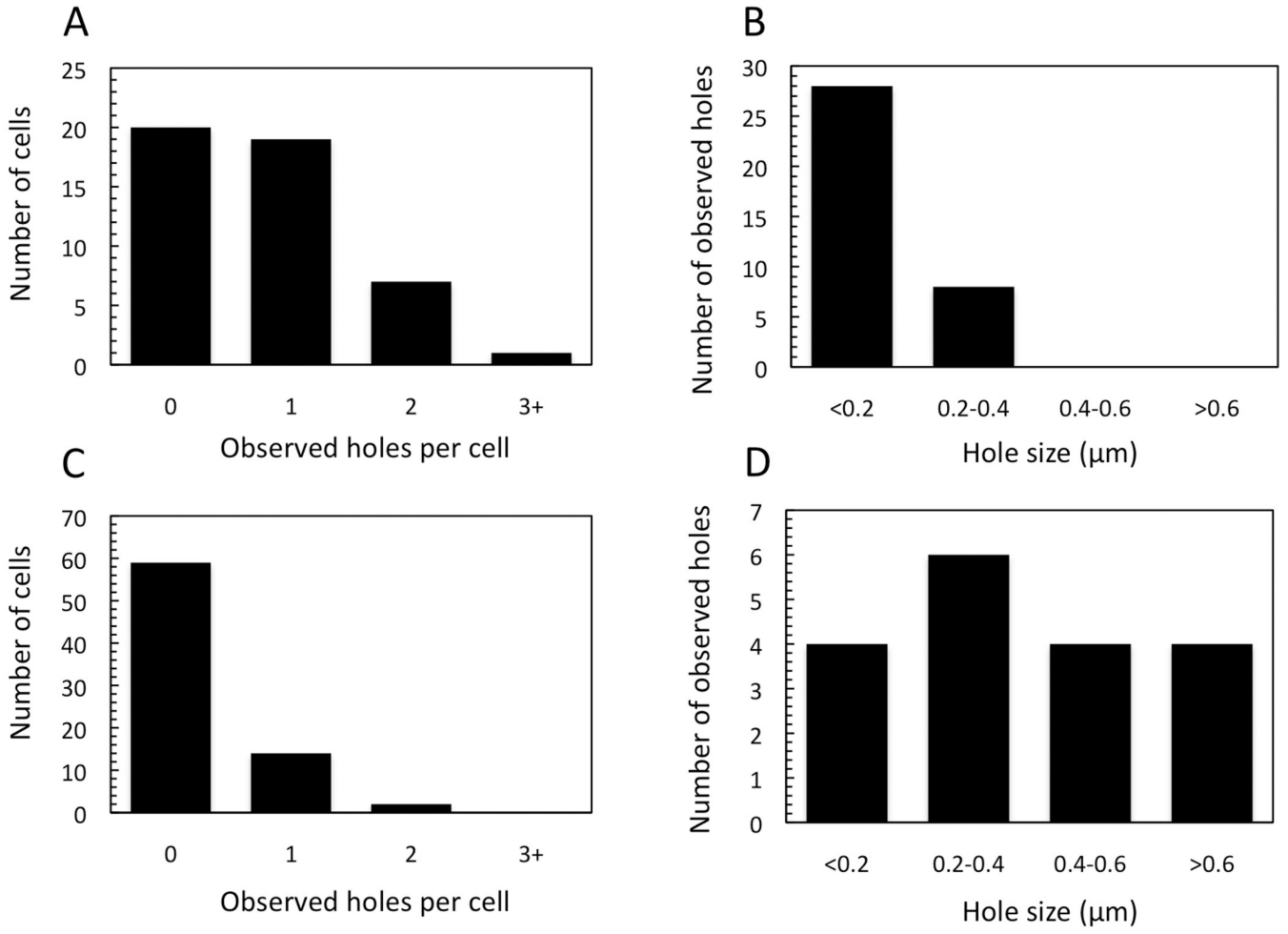

Figure 4.

Early triggering by $S105_{A52F}$ or by S105 wt with the addition of KCN. *E. coli* MC4100 Δ*tonA* λCamΔ*SR* carrying either $pS105R_{am}Rz_{am}Rz1_{am}$ or an isogenic plasmid with the *$S105_{A52F}$* allele were thermally induced and KCN was added to the former culture 15 minutes later. Cells were plunge frozen and imaged as described for Fig. 2. (A) Number of holes/cell observed and (B) hole size distribution for $S105_{A52F}$. (C) Number of holes/cell and (D) hole size distribution for wt S105 prematurely triggered with KCN.

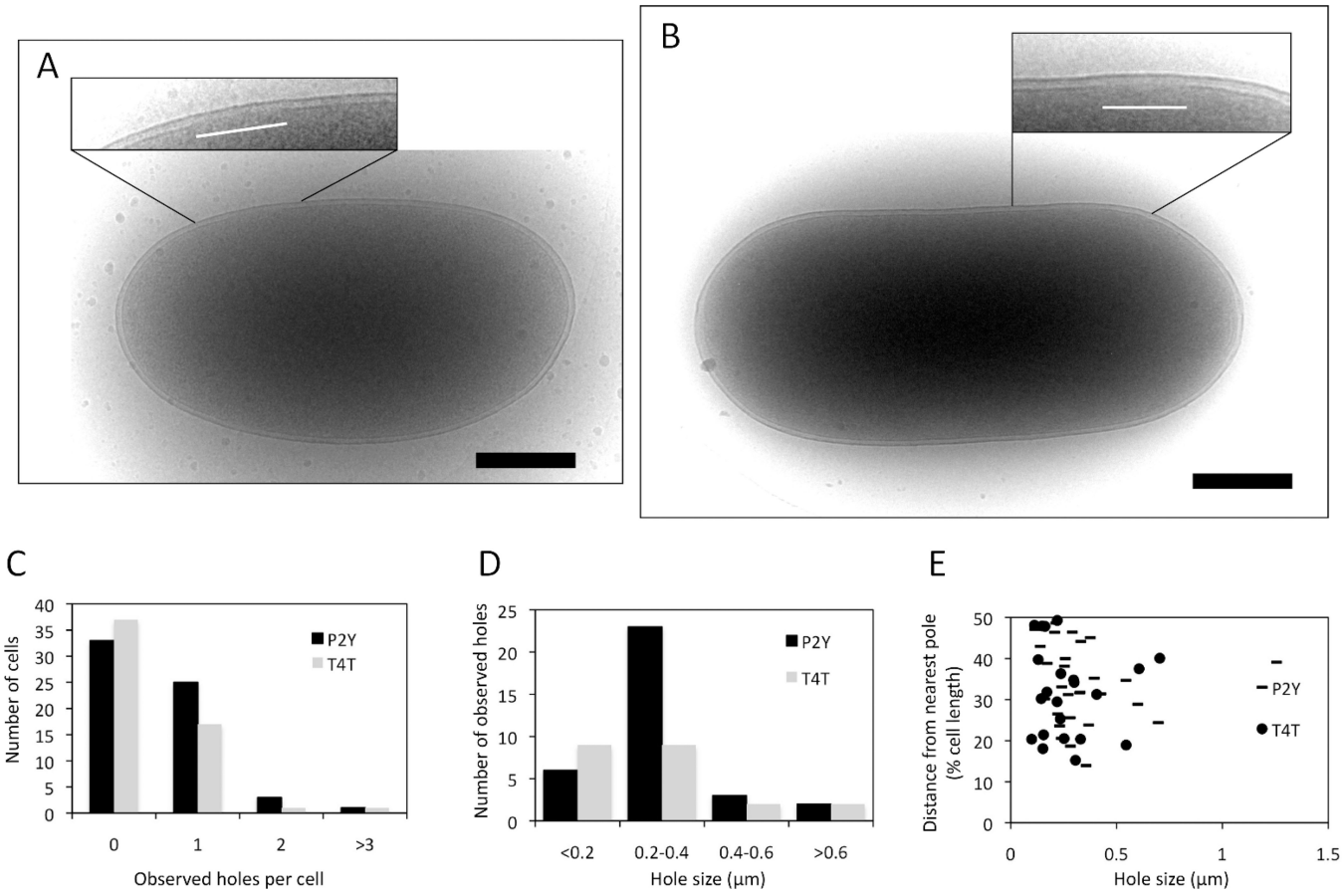

Figure 5.

Hole formation by different holins. (A) *E. coli* MC4100 Δ*tonA* λCamΔ*SR* cells carrying a plasmid isogenic to pS105$R_{am}Rz_{am}Rz1_{am}$ but with the indicated heterologous holin gene substituted for *S105* were thermally induced, sampled and analyzed as described for Fig. 2. (A) P2 *Y*; (B) T4 *t*. Insets: close-up views of the areas in which inner membrane lesions are observed. The white lines indicate the location and extent of the lesions Scale bars correspond to 500 nm. (C) Number of holes/cell for P2 Y and T4 T. (D) Hole size distribution for P2 Y and T4 T. (E) Hole distance from nearest pole for P2 Y and T4 T.